Electronic Absorption Spectra of the Polyacetylene Chains $HC_{2n}H$, $HC_{2n}H^-$, and $HC_{2n-1}N^-$ ($n = 6-12$) in Neon Matrixes

M. Grutter, M. Wyss, J. Fulara, and J. P. Maier*

Institute for Physical Chemistry, University of Basel, Klingelbergstrasse 80, CH-4056 Basel, Switzerland

Received: July 28, 1998; In Final Form: September 23, 1998

Three electronic transitions of the isoelectronic species $HC_{2n}H^-$ and $HC_{2n-1}N^-$ and one of the neutral polyacetylenes $HC_{2n}H$ ($n = 6-12$) have been observed by absorption spectroscopy in neon matrixes. Anions produced in an electron impact source were mass-selected and codeposited with excess of neon at 6 K. The $HC_{2n}H$ species were formed from the anions by photodetachment. A well-structured band system at 780 nm for $HC_{12}H^-$, and shifting by regular increments to 1325 nm for $HC_{24}H^-$, is assigned to two overlapping electronic transitions of $^2\Pi \leftarrow X^2\Pi$ symmetry. Another $^2\Pi \leftarrow X^2\Pi$ transition with broader features is observed in the 300−480 nm region. Corresponding transitions are observed for the isoelectronic cyanosubstituted anions $HC_{2n-1}N^-$. The neutral polyacetylenes show a vibrationally well-resolved UV band system attributed to the $^1\Sigma_u^+ \leftarrow X^1\Sigma_g^+$ electronic transition. The energy of the electronic transition shows a characteristic inverse dependence on the carbon chain length.

1. Introduction

Polyacetylenes are of relevance in the chemistry of dense interstellar clouds and may serve as intermediates in the formation of polyaromatic hydrocarbons and fullerenes.[1] The $HC_{2n+1}N$ ($n = 0-5$)[2] and $C_{2n}H$ ($n = 1-4$)[3] polyynes include the largest linear molecules identified in space. The presence of cumulenic chains H_2C_n ($n = 3, 4, 6$) in the interstellar medium[4] has also been established from their microwave spectra.[5] The absence of a permanent dipole moment in the isomeric polyacetylenic chains $H-(C{\equiv}C)_n-H$ hinders their detection by radio astronomy although they are expected to be similarly abundant.[6,7] The smallest members, HC_2H and HC_4H, have been identified in Titan's atmosphere by infrared spectroscopy.[8]

Long polyacetylenes show surprising stability at high temperatures according to thermodynamic studies.[9] The addition of small amounts of H_2 and H_2O to laser-vaporized graphite provided evidence that C_nH_2 ($n = 10-20$) molecules are predominantly linear.[10] The mass patterns indicate that these are polyynes, and compared to that of bare carbon chains, the linear isomer range is considerably extended. Another laser desorption study,[11] which produced mixed carbon/hydrogen cations $C_nH_x^+$ ($x = 0-15$, $n = 5-22$), led to the conclusion that the polyacetylenic structure dominates for $n =$ even, $x = 2$, and that the linear form extends up to $n \geq 22$. Because the hydrogens act as electron donors, a similar structure pattern should hold for their anions $C_nH_x^-$. Cumulenic structures are expected for $n =$ odd either with both hydrogens on one end or as biradicals. These predictions agree with collision-induced-dissociation studies on $C_nH_2^-$.[12]

Electronic transitions of several series of carbon chains have been observed in inert gas matrixes and in the gas phase.[13] The spectra of the polyacetylenes, $HC_{2n}H$, have been recorded for $n = 1-4$ in the gas phase[14] and for $n = 4-12$ in solution,[15] and those for $HC_{2n+1}H$ ($n = 2-7$) after mass-selected codeposition in neon.[16] In case of the cations, $HC_{2n}H^+$ ($n = 2-4$), the $A^2\Pi \rightarrow X^2\Pi$ band systems have been observed in the gas phase as emission spectra.[17] The absorption spectra of these electronic transitions were also measured for $HC_{2n}H^+$ ($n = 2-8$) and $HC_{2n+1}H^+$ ($n = 2-7$) in neon matrixes.[18]

Little is known experimentally about the anions although HC_6H^- has been calculated to have $^2\Pi_g$ symmetry in the ground state.[19] In this contribution, the electronic absorption spectra in neon matrixes of anionic and neutral polyacetylenic chains with up to 24 carbon atoms, as well as of their isoelectronic $HC_{2n-1}N^-$ counterparts, are presented.

2. Experimental Section

The apparatus combining mass selection and matrix isolation spectroscopy has been described.[20] A hot-cathode anion source was fed with a diacetylene−argon mixture (1:3) to produce the polyacetylenes. The ions were extracted with 200 eV energy and led via a 90° deflector into a quadrupole filter. The mass-selected ions were then codeposited with neon at 6 K on a rhodium-coated sapphire plate during ≈2 h.

At a source pressure of $\approx 10^{-4}$ mbar, mainly the species $C_{2n}H_x^-$ ($x = 2$) are formed for $n \geq 5$. The smaller unsaturated chains are predominantly monohydrated, and for $n \geq 9$, the $x = 4$ peak becomes noticeable in the mass spectrum. Depositions with a mass resolution of ±1 u can be carried out for $C_{12}H_2^-$ and $C_{14}H_2^-$ where the ion current (20 and 10 nA, respectively) is still large enough for optical detection. The resolution was degraded to ±5 u for the larger species; the ion current dropped from 5 nA for $C_{16}H_x^-$ to 0.4 nA for $C_{24}H_x^-$. Chains with odd number of carbons are produced inefficiently in the source.

The cyanopolyacetylene anions were produced by the introduction of HCCCN into the mixture at a concentration giving the correct C:N ratio for the molecule size of interest; e.g., HC_4H:$HC_3N \approx 2:1$ to produce $HC_{11}N^-$. Ion currents similar to those for the polyacetylenes were obtained by allowing depositions of $HC_{11}N^-$ and $HC_{13}N^-$ to be carried out at a mass resolution of ±1 u.

Absorption spectra were measured in the 220−1100 nm region with the waveguide technique[21] using monochromatic

10.1021/jp983185t CCC: $15.00
Published on Web 11/10/1998

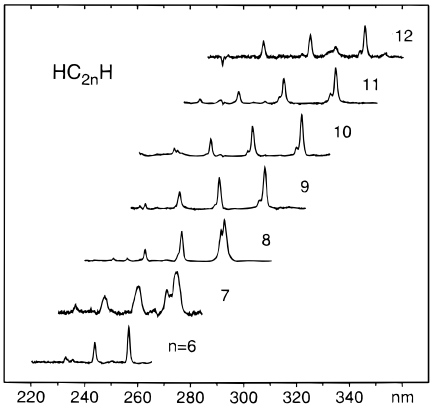

Figure 1. The $^1\Sigma_u^+ \leftarrow X^1\Sigma_g^+$ electronic transition of the neutral polyacetylenic chains $HC_{2n}H$ in 6 K neon matrixes. The spectra were obtained after codeposition of mass-selected anions with neon and subsequent electron detachment with a mercury arc lamp ($\lambda \leq 400$ nm).

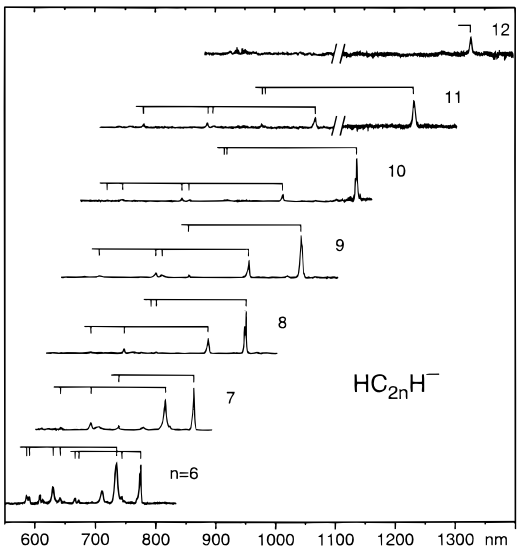

Figure 2. Spectra of the $HC_{2n}H^-$ anionic chains ($n = 6-12$) showing the overlapping (1) $^2\Pi \leftarrow X^2\Pi$ and (2) $^2\Pi \leftarrow X^2\Pi$ electronic transitions observed in 6 K neon matrixes. The spectral region above 1100 nm is inaccessible with the more sensitive waveguide method and was therefore measured with a single reflection of an FTIR beam and an InSb detector.

light from xenon arc and halogen light sources. A Fourier transform spectrometer was used below 9000 cm^{-1} in a single-reflection configuration.[22] The matrixes were in all cases irradiated with a 150 W mercury lamp for approximately 30 min using various cutoff filters to produce the neutral polyacetylenes by electron detachment.

3. Results and Discussion

3.1. Electronic Transitions of $HC_{2n}H$, $n = 6-12$. Several absorption features are observed after mass-selected codeposition of $C_{2n}H_x^-$ ($n = 6-12$) anions with neon at 6 K. Structured band systems in the UV and near-infrared regions are apparent (Figures 1 and 2). A third band system with broad absorption features (Figure 3) is seen in the 300−450 nm region. All systems shift progressively to longer wavelength as the size of the chain increases.

The near-infrared and UV absorptions seen in Figures 2 and 3 disappear after the matrix is illuminated with ≥3 eV photons. At the same time, the absorption bands in Figure 1 grow in

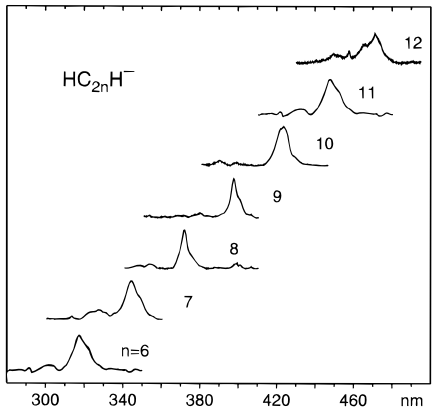

Figure 3. The (3) $^2\Pi \leftarrow X^2\Pi$ electronic transition observed for the $HC_{2n}H^-$ anionic chains in 6 K neon matrixes.

intensity. It could be established in measurements on the smallest members of the series using higher mass resolution that the absorbers contain two hydrogens. Even though fragmentation can take place with ∼200 eV kinetic energy of the ions, deposition of, for example, $C_{12}H_2^-$ shows only weakly the known electronic transitions of $C_{12}H$[20] and C_{12}^-,[23] whereas selection of $C_{12}H^-$ leads to strong $C_{12}H$ signals and absence of the bands seen in Figure 1. These systems could also be observed for the smaller members of the series using the hot-cathode source employed previously to measure the $A^2\Pi \leftarrow X^2\Pi$ electronic transitions of the $H-(C{\equiv}C)_n-H^+$ chains[18] and subsequent neutralization.

The wavelengths of the origin bands are plotted in Figure 4 (bottom) along with the data from measurements on polyacetylene chains in methanol.[15] A regular shift between the band maxima observed in solution and in neon is evident; this increases from 15 nm for $HC_{12}H$ to 30 nm for $HC_{24}H$. The $^1\Sigma_u^+ \leftarrow X^1\Sigma_g^+$ electronic transitions of $H-(C{\equiv}C)_n-H$ ($n = 2-4$) have been measured in the gas-phase.[14] There is a close correpondence in the wavelength dependence between gas-phase

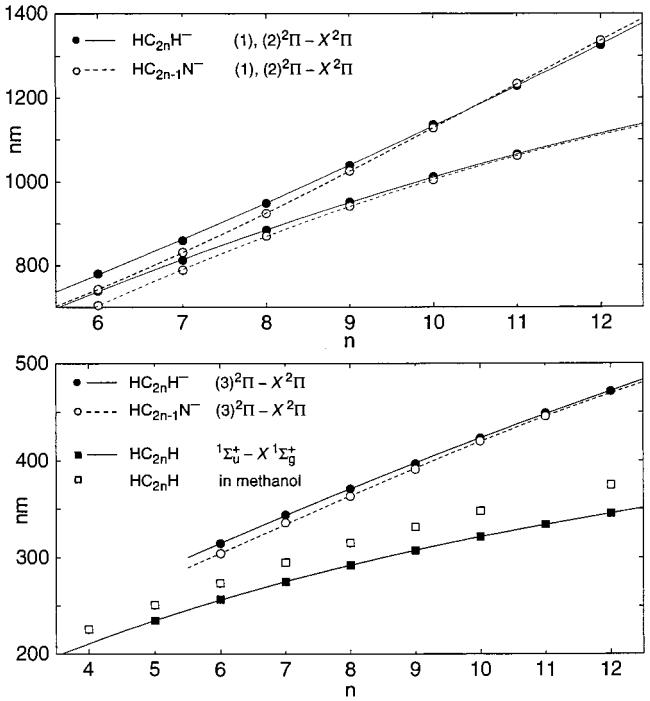

Figure 4. Wavelength dependence of the electronic transitions (origin bands) of polyacetylenic anions and neutrals on their size. The values for the $HC_{2n}H$ molecules measured in methanol are from ref 15.

TABLE 1: Observed Bands (Maxima ±0.2 nm) for the $^1\Sigma_u^+ \leftarrow X^1\Sigma_g^+$ Electronic Transitions of $HC_{2n}H$ ($n = 6-12$) in 6 K Neon Matrixes

λ (nm)	ν (cm^{-1})	$\Delta\nu$ (cm^{-1})	assignment
256.6	38 971	0	$HC_{12}H$ 0_0^0
243.9	41 000	2029	ν(C≡C str)
232.8	42 955	3984	2ν(C≡C)
274.9	36 377	0	$HC_{14}H$ 0_0^0
271.1	36 887	510	
260.3	38 417	2040	ν(C≡C str)
247.5	40 404	4027	2ν(C≡C)
236.5	42 283	5906	3ν(C≡C)
292.2	34 223	0	$HC_{16}H$ 0_0^0
291.0	34 364	141	
276.1	36 219	1996	ν(C≡C str)
262.2	38 139	3916	2ν(C≡C)
250.3	39 952	5729	3ν(C≡C)
307.3	32 541	0	$HC_{18}H$ 0_0^0
305.4	32 744	202	
290.2	34 459	1918	ν(C≡C str)
275.3	36 324	3783	2ν(C≡C)
262.2	38 139	5597	3ν(C≡C)
321.4	31 114	0	$HC_{20}H$ 0_0^0
319.4	31 309	195	
302.8	33 025	1911	ν(C≡C str)
301.2	33 201	2087	ν(C≡C) + ν(195)
287.1	34 831	3717	2ν(C≡C)
273.4	36 576	5463	3ν(C≡C)
334.2	29 922	0	$HC_{22}H$ 0_0^0
332.2	30 102	180	
314.6	31 786	1864	ν(C≡C str)
297.6	33 602	3680	2ν(C≡C)
283.0	35 336	5413	3ν(C≡C)
270.6	36 955	7033	4ν(C≡C)
345.4	28 952	0	$HC_{24}H$ 0_0^0
343.4	29 121	169	
324.7	30 798	1846	ν(C≡C str)
306.9	32 584	3632	2ν(C≡C)

excitation energies[14] extrapolated for the longer chains and the actual observations in neon matrixes.

The above trends and comparison of the vibrational patterns in these three environments indicate that the spectra in Figure 1 are the $^1\Sigma_u^+ \leftarrow X^1\Sigma_g^+$ transitions of the linear H−(C≡C)$_n$−H species. In Table 1 the bands which are considered to belong to these systems are listed.

3.2. Electronic Transitions of $HC_{2n}H^-$, $n = 6-12$. The two absorption systems which can be bleached on irradiation with wavelengths below 400 nm are seen in Figures 2 and 3. Figure 5 shows the absorption system of $HC_{12}H^-$ in more detail. There are two strong bands close to each other. The one at 780 nm shows distinct site structure whereas that at 739 nm is featureless and broader. These absorptions belong to the same species because the intensity ratios of the bands are constant in different experiments and selective wavelength irradiation does not discriminate any of the bands.

The shapes of the two peaks, the vibrational patterns discernible, and the Franck−Condon factors indicate that the 780 and 739 nm bands are origins of two different electronic transitions. The progressions discernible have the same band shapes as their respective origin band. It is supposed that the lower energy one is the (1) $^2\Pi \leftarrow X^2\Pi$ transition. Extrapolation of the observed low-energy band origins down to HC_6H^- gives 2.1 eV, which is comparable to the calculated value of 2.67 eV.[19] The higher energy band system is an electronic transition probably also of $^2\Pi \leftarrow X^2\Pi$ symmetry due to its intensity. As can be seen in Figure 2, the two origins move apart with size, reaching a spacing of over 1200 cm^{-1} for the largest members, and at the same time the higher energy peak loses intensity. This suggests that there are vibronic interactions between these transitions which are larger for the smaller species because the states are energetically closer. The pronounced interactions are revealed by the complexity of the $HC_{12}H^-$ spectrum.

A second strong band system is detected in the UV region (Figure 3). This absorption correlates in intensity with the lower lying electronic transitions on irradiation. Wavelength-selective photolysis leads to an estimate of ∼1.5 eV for the gas-phase electron detachment threshold of $HC_{12}H^-$ when ≈1 eV solvation energy of the anions in the neon environment is taken into account. This implies that the third excited electronic state of the $HC_{2n}H^-$ anion, i.e., the upper state of the absorptions seen in Figure 3, lies above the gas-phase electron affinity of the corresponding neutral polyacetylene, leading to considerable broadening.

The plot in Figure 4 (top, near-infrared; bottom, UV) shows a regular shift of the states to longer wavelength as the size of the chain increases, characteristic of $\pi-\pi$ electron excitations.[24] The absorption systems are labeled in Table 2 as the (1), (2), and (3) $^2\Pi \leftarrow X^2\Pi$ electronic transitions of the $HC_{2n}H^-$ chains. Progressions of ∼2000 cm^{-1}, typical for C≡C stretching modes, are observed up to $HC_{22}H^-$ for the two lower electronic transitions. The vibrational frequencies observed are somewhat different in both states. In view of the anion to neutral conversion upon photolysis and comparison to the related $HC_{2n-1}N^-$ species (section 3.3), the possibility that the absorbers have a cumulenic structure with both hydrogens on one end is disregarded.

In the infrared region, two bands at 1964.1 and 1898.2 cm^{-1} are observed after mass selection of $HC_{12}H^-$. These peaks correlate in intensity and irradiation behavior with the electronic transitions attributed to $HC_{12}H^-$. A band at 1920.2 cm^{-1} is observed for $HC_{14}H^-$. These are frequencies which could be expected for asymmetric C≡C streching vibrations. No infrared bands could be detected for the longer chains.

3.3. Electronic Transitions of $HC_{2n-1}N^-$, $n = 6-11$. On addition of cyanoacetylene to the mixture in the ion source, the most evident change in the mass spectrum is the increase in intensity of the peak 1 u higher to that of $C_{2n}H_2^-$. The formation of $HC_{2n-1}N^-$ is the main contributor to this change. Figure 6 shows the absorption spectra in the near-infrared region following mass-selected deposition of the $HC_{2n-1}N^-$ species.

After deposition of $HC_{11}N^-$ with unity mass resolution, very little of $HC_{12}H^-$ was present, as can be seen by comparing the two spectra in Figure 5. The observed system clearly resembles that of $HC_{12}H^-$ and is slightly blue-shifted. Absorption features in the $HC_{11}N^-$ spectrum such as the sharp peak at lower energy

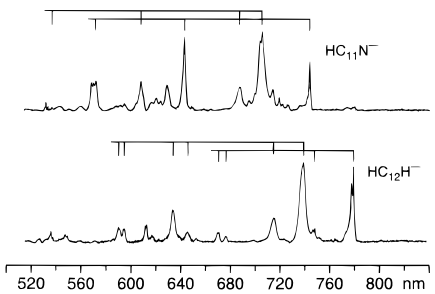

Figure 5. The overlapping (1) $^2\Pi \leftarrow X^2\Pi$ and (2) $^2\Pi \leftarrow X^2\Pi$ electronic transitions of the isoelectronic $HC_{12}H^-$ and $HC_{11}N^-$ chains. The spectra were recorded after codeposition of the anions with unity mass resolution in neon at 6 K.

TABLE 2: Observed Bands (Maxima ±0.2 nm) for the (1) $^2\Pi \leftarrow X^2\Pi$, (2) $^2\Pi \leftarrow X^2\Pi$, and (3) $^2\Pi \leftarrow X^2\Pi$ Electronic Transitions of $HC_{2n}H^-$ ($n = 6-12$) in 6 K Neon Matrixes

λ (nm)	ν (cm^{-1})	$\Delta\nu$ (cm^{-1})	assignment	$\Delta\nu$ (cm^{-1})	assignment
			$HC_{12}H^-$		
780.4	12 814	0	(1) $^2\Pi_g \leftarrow X^2\Pi_u\ 0_0^0$		
748.3	13 364	550	ν(C−C str)		
739.3	13 526			0	(2) $^2\Pi_g \leftarrow X^2\Pi_u\ 0_0^0$
714.8	13 990			464	ν(C−C str)
675.3	14 808	1994	ν(C≡C str)		
668.7	14 954	2140	ν(C≡C str)		
650.8	15 366	2552	$\nu(2140) + \nu(550)$		
643.5	15 540			2014	ν(C≡C str)
631.8	15 828			2301	ν(C≡C str)
614.8	16 265			2739	$\nu(2301) + \nu(464)$
591.5	16 906			3380	ν(C−H str)
587.2	17 030			3504	
567.4	17 624			4098	
543.2	18 409			4883	
522.2	19 150			5623	
317.4	31 506		(3) $^2\Pi_g \leftarrow X^2\Pi_u\ 0_0^0$		
			$HC_{14}H^-$		
859.6	11 633	0	(1) $^2\Pi_u \leftarrow X^2\Pi_g\ 0_0^0$		
820.2	12 192	559			
812.4	12 309			0	(2) $^2\Pi_u \leftarrow X^2\Pi_g\ 0_0^0$
775.2	12 900			591	
734.8	13 609	1976	ν(C≡C str)		
689.0	14 514			2205	ν(C≡C str)
639.2	15 645			3335	ν(C−H str)
344.0	29 070		(3) $^2\Pi_u \leftarrow X^2\Pi_g\ 0_0^0$		
			$HC_{16}H^-$		
948.8	10 540	0	(1) $^2\Pi_g \leftarrow X^2\Pi_u\ 0_0^0$		
884.9	11 301			0	(2) $^2\Pi_g \leftarrow X^2\Pi_u\ 0_0^0$
798.6	12 522	1982	ν(C≡C str)		
790.2	12 655	2115	ν(C≡C str)		
745.0	13 423			2122	ν(C≡C str)
690.1	14 491			3190	ν(C−H str)
371.2	26 940		(3) $^2\Pi_g \leftarrow X^2\Pi_u\ 0_0^0$		
			$HC_{18}H^-$		
1038.9	9 626	0	(1) $^2\Pi_u \leftarrow X^2\Pi_g\ 0_0^0$		
951.8	10 506			0	(2) $^2\Pi_u \leftarrow X^2\Pi_g\ 0_0^0$
851.3	11 747	2121	ν(C≡C str)		
806.3	12 402			1896	ν(C≡C str)
796.5	12 555			2049	ν(C≡C str)
702.1	14 243			3737	$\nu(2049) + \nu(1896)$
367.0	27 248		(3) $^2\Pi_u \leftarrow X^2\Pi_g\ 0_0^0$		
			$HC_{20}H^-$		
1135.2	8 809	0	(1) $^2\Pi_g \leftarrow X^2\Pi_u\ 0_0^0$		
1011.4	9 887			0	(2) $^2\Pi_g \leftarrow X^2\Pi_u\ 0_0^0$
918.3	10 890	2081	ν(C≡C str)		
914.4	10 936	2127	ν(C≡C str)		
854.5	11 703			1815	ν(C≡C str)
842.2	11 874			1986	ν(C≡C str)
743.0	13 459			3572	$\nu(1986) + \nu(1815)$
718.9	13 910			4023	$2\nu(1986)$
423.1	23 635		(3) $^2\Pi_g \leftarrow X^2\Pi_u\ 0_0^0$		
			$HC_{22}H^-$		
1228.6	8 139	0	(1) $^2\Pi_u \leftarrow X^2\Pi_g\ 0_0^0$		
1064.6	9 393			0	(2) $^2\Pi_u \leftarrow X^2\Pi_g\ 0_0^0$
980.0	10 204	2065	ν(C≡C str)	811	
974.9	10 257	2118	ν(C≡C str)	864	
913.8	10 943	2804		1550	
894.3	11 182			1789	ν(C≡C str)
884.0	11 312			1919	ν(C≡C str)
777.7	12 858			3465	$\nu(1919) + \nu(1789)$
448.8	22 282		(3) $^2\Pi_u \leftarrow X^2\Pi_g\ 0_0^0$		
			$HC_{24}H^-$		
1325.3	7 545		(1) $^2\Pi_g \leftarrow X^2\Pi_u\ 0_0^0$		
471.3	21 218		(3) $^2\Pi_g \leftarrow X^2\Pi_u\ 0_0^0$		

TABLE 3: Observed Bands (Maxima ±0.2 nm) for the (1) $^2\Pi \leftarrow X^2\Pi$, (2) $^2\Pi \leftarrow X^2\Pi$ and (3) $^2\Pi \leftarrow X^2\Pi$ Electronic Transitions of $HC_{2n-1}N^-$ ($n = 6-11$) in 6 K Neon Matrixes

λ (nm)	ν (cm^{-1})	$\Delta\nu$ (cm^{-1})	assignment	$\Delta\nu$ (cm^{-1})	assignment
			$HC_{11}N^-$		
742.6	13 466	0	(1) $^2\Pi \leftarrow X^2\Pi\ 0_0^0$		
724.9	13 795	329			
717.9	13 930	463			
712.8	14 029	563			
704.4	14 196			0	(2) $^2\Pi \leftarrow X^2\Pi\ 0_0^0$
693.5	14 420			223	
686.1	14 575			379	
641.7	15 584	2117	ν(C≡C str)		
627.4	15 939	2473		1742	
618.4	16 171			1974	ν(C≡C str)
606.3	16 493			2297	ν(C≡C str)
593.0	16 863	3397		2667	
570.3	17 535	4068		3338	ν(C−H str)
568.3	17 596	4130		3400	
566.7	17 646	4180	2ν(2117)	3450	
534.9	18 695			4499	2ν(2297)
304.0	32 895		(3) $^2\Pi \leftarrow X^2\Pi\ 0_0^0$		
			$HC_{13}N^-$		
830.7	12 038	0	(1) $^2\Pi \leftarrow X^2\Pi\ 0_0^0$		
800.6	12 491	453			
787.9	12 692			0	(2) $^2\Pi \leftarrow X^2\Pi\ 0_0^0$
711.4	14 057	2019	ν(C≡C str)	1365	
685.2	14 594			1902	ν(C≡C str)
672.7	14 865			2173	ν(C≡C str)
624.3	16 018			3326	ν(C−H str)
336.0	29 762		(3) $^2\Pi \leftarrow X^2\Pi\ 0_0^0$		
			$HC_{15}N^-$		
925.0	10 811	0	(1) $^2\Pi \leftarrow X^2\Pi\ 0_0^0$		
914.6	10 934	123			
869.6	11 500			0	(2) $^2\Pi \leftarrow X^2\Pi\ 0_0^0$
734.5	13 615			2115	ν(C≡C str)
363.3	27 525		(3) $^2\Pi \leftarrow X^2\Pi\ 0_0^0$		
			$HC_{17}N^-$		
1026.2	9 745	0	(1) $^2\Pi \leftarrow X^2\Pi$		
942.4	10 611			0	(2) $^2\Pi \leftarrow X^2\Pi\ 0_0^0$
842.5	11 869	2125	ν(C≡C str)		
789.8	12 661			2050	ν(C≡C str)
391.2	25 562		(3) $^2\Pi \leftarrow X^2\Pi\ 0_0^0$		
			$HC_{19}N^-$		
1128.2	8 864	0	(1) $^2\Pi \leftarrow X^2\Pi\ 0_0^0$		
1005.0	9 950			0	(2) $^2\Pi \leftarrow X^2\Pi\ 0_0^0$
909.9	10 990	2127	ν(C≡C str)		
849.6	11 770			1820	
839.2	11 916			1966	ν(C≡C str)
420.1	23 804		(3) $^2\Pi \leftarrow X^2\Pi\ 0_0^0$		
			$HC_{21}N^-$		
1233.3	8 108	0	(1) $^2\Pi \leftarrow X^2\Pi\ 0_0^0$		
1062.4	9 413			0	(2) $^2\Pi \leftarrow X^2\Pi\ 0_0^0$
979.9	10 205	2097	ν(C≡C str)		
975.5	10 251	2143	ν(C≡C str)		
891.6	11 216			1803	
883.5	11 319			1906	ν(C≡C str)
776.5	12 878			3466	
445.7	22 437		(3) $^2\Pi \leftarrow X^2\Pi\ 0_0^0$		
			$HC_{23}N^-$		
1336.3	7 483		(1) $^2\Pi \leftarrow X^2\Pi\ 0_0^0$		
345.4	28 952		(3) $^2\Pi \leftarrow X^2\Pi\ 0_0^0$		

and the broad band with greatest intensity reflect the pattern in the $HC_{12}H^-$ system. Consequently, the band systems are also assigned to two nearby $^2\Pi \leftarrow X^2\Pi$ electronic transitions.

Due to insufficient mass resolution during the deposition of the longer chains, the spectra initially showed the bands belonging to $HC_{2n}H^-$ (section 3.2) as well as overlapping new absorptions in both the near-infrared and the UV regions. However, irradiation of the matrix with selected wavelengths

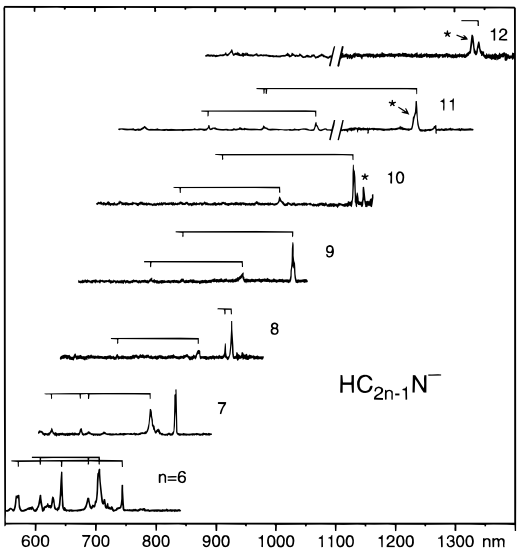

Figure 6. Spectra showing the overlapping (1) $^2\Pi \leftarrow X^2\Pi$ and (2) $^2\Pi \leftarrow X^2\Pi$ electronic transitions of the $HC_{2n-1}N^-$ ($n = 6-12$) anionic chains measured in 6 K neon matrixes. The matrixes were irradiated with filters of selected wavelengths to partially eliminate absorptions due to the $HC_{2n}H^-$ anions (marked with asterisks).

led to photobleaching of the $HC_{2n}H^-$ absorptions, leaving those due to $HC_{2n-1}N^-$ because the latter anions have larger detachment energies. Absorption spectra of $HC_{13}N^-$ and $HC_{15}N^-$ without the polyacetylene anions were obtained with $\lambda \geq 365$ nm irradiation (Figure 6). Photons with $\lambda \geq 345$ nm were needed to eliminate $HC_{18}H^-$ absorptions from those of $HC_{17}N^-$. Larger species proved more difficult to separate; all of these polyynes with more than 20 heavy atoms have gas-phase electron affinities larger than 3 eV.

A list of the bands observed and assigned to the $HC_{2n-1}N^-$ chains ($n = 6-12$), including a broad UV band system (not shown in figure) equivalent to the $HC_{2n}H^-$ absorptions (Figure 4), is given in Table 3. The $^1\Sigma_u^+ \leftarrow X^1\Sigma_g^+$ transitions of the neutral cyanopolyacetylenes are also expected in the 250−350 nm region. A variety of absorptions are observed, but due to overlap, definite assignments could not be made.

4. Conclusions

Electronic transitions of $HC_{2n}H$, $HC_{2n}H^-$, and $HC_{2n-1}N^-$ ($n = 6-12$) have been measured in neon matrixes. The detection of these long, highly unsaturated carbon chains proves that the range of the linear, or quasi-linear, structure of the carbon backbone is considerably extended by the terminal hydrogens and cyano group. Electronic transitions of bare and monohydrogenated carbon chains with even numbers of carbon atoms have only been detected up to C_{10}[23] and $C_{16}H$[20] whereas in the polyacetylenes up to $HC_{24}H$ and $HC_{24}H^-$ are observed. The location and identification of the electronic transitions of these long carbon chains provide the necessary data for their characterization in the gas phase.

Acknowledgment. This work is part of Project No. 20-49104.96 of the Swiss National Science Foundation.

References and Notes

(1) Bohme, D. K. *Chem. Rev.* **1992**, *92*, 1487.
(2) Bell, M. B.; Feldman, P. A.; Travers, M. J.; McCarthy, M. C.; Gottlieb, C. A.; Thaddeus, P. *Astrophys. J.* **1997**, *483*, L61.
(3) Cernicharo, J.; Guélin, M. *Astron. Astrophys.* **1996**, *309*, L27.
(4) Langer, W. D.; Velusamy, T.; Kuiper, T. B. H.; Peng, R.; McCarthy, M. C.; Travers, M. J.; Kovács, A.; Gottlieb, C. A.; Thaddeus, P. *Astrophys. J. Lett.* **1997**, *480*, L63.
(5) McCarthy, M. C.; Travers, M. J.; Kovács, A.; Gottlieb, C. A.; Thaddeus, P. *Astrophys. J., Suppl. Ser.* **1997**, *113*, 105.
(6) Cherchneff, I.; Glassgold, A. E. *Astrophys. J.* **1993**, *419*, L41.
(7) Thaddeus, P.; McCarthy, M. C.; Travers, M. J.; Gottlieb, C. A.; Chen, W. *Faraday Discuss.* **1998**, *109*, 121.
(8) Kunde, V. G.; Aikin, A. C.; Hanel, R. A.; Jennings, D. E.; Maguire, W. C.; Samuelson, R. E. *Nature* **1981**, *292*, 686.
(9) Stein, S. E.; Fahr, A. *J. Phys. Chem.* **1985**, *89*, 3714.
(10) Heath, J. R.; Zhang, Q.; O'Brien, S. C.; Curl, R. F.; Kroto, H. W.; Smalley, R. E. *J. Am. Chem. Soc.* **1987**, *109*, 359.
(11) Lee, S.; Gotts, N.; von Helden, G.; Bowers, M. T. *J. Phys. Chem. A.* **1997**, *101*, 2096.
(12) Jiao, C.; Phelps, D. K.; Lee, S.; Huang, Y.; Freiser, B. S. *Rapid Commun. Mass Spectrom.* **1993**, *7*, 404.
(13) Maier, J. P. *J. Phys. Chem. A* **1998**, *102*, 3462.
(14) Kloster-Jensen, E.; Haink, H. J.; Christen, H. *Helv. Chim. Acta* **1974**, *57*, 1731.
(15) Eastmond, R.; Johnson, T. R.; Walton, D. R. M. *Tetrahedron* **1972**, *28*, 4601.
(16) Fulara, J.; Freivogel, P.; Forney, D.; Maier, J. P. *J. Chem. Phys.* **1995**, *103*, 8805.
(17) Klapstein, D.; Kuhn, R.; Maier, J. P.; Ochsner, M.; Zambach, W. *J. Phys. Chem.* **1984**, *88*, 5176.
(18) Freivogel, P.; Fulara, J.; Lessen, D.; Forney, D.; Maier, J. P. *Chem. Phys.* **1994**, *189*, 335.
(19) Sobolewski, A. L.; Adamowicz, L. *J. Chem. Phys.* **1995**, *102*, 394.
(20) Freivogel, P.; Fulara, J.; Jakobi, M.; Forney, D.; Maier, J. P. *J. Chem. Phys.* **1995**, *103*, 54.
(21) Rossetti, R.; Brus, L. E. *Rev. Sci. Instrum.* **1980**, *51*, 467.
(22) Forney, D.; Fulara, J.; Freivogel, P.; Jakobi, M.; Lessen, D.; Maier, J. P. *J. Chem. Phys.* **1995**, *103*, 48.
(23) Freivogel, P.; Grutter, M.; Forney, D.; Maier, J. P. *J. Chem. Phys.* **1997**, *107*, 4468.
(24) Forney, D.; Grutter, M.; Freivogel, P.; Maier, J. P. *J. Phys. Chem. A* **1997**, *101*, 5292.